#156

Phys Chem Minerals (1993) 19:357–360

Papers from the GEOPHYSICAL LABORATORY
Carnegie Institution of Washington NO. 2306

PHYSICS AND CHEMISTRY OF MINERALS

Phase E: A High Pressure Hydrous Silicate with Unique Crystal Chemistry

Y. Kudoh [1,*], L.W. Finger [1], R.M. Hazen [1], C.T. Prewitt [1], M. Kanzaki [2,], and D.R. Veblen [3]**

[1] Geophysical Laboratory, Carnegie Institution of Washington, Washington, DC 20015, USA
[2] Department of Geology, University of Alberta, Edmonton T6G 2E3, Canada
[3] Department of Earth and Planetary Sciences, Johns Hopkins University, Baltimore, MD 21218, USA

Received March 9, 1992 / Revised, accepted July 21, 1992

Abstract. The unique cation-disordered crystal structures of two samples of phase E, a non-stoichiometric, hydrous silicate synthesized in a uniaxial, split-sphere, multi-anvil apparatus at conditions above 13 GPa and 1000° C, have been solved and refined in space group $R\bar{3}m$. The compositions and unit cells for the two materials, assuming six oxygens per cell, are $Mg_{2.08}Si_{1.16}H_{3.20}O_6$, a = 2.9701(1) Å, c = 13.882(1) Å, V = 106.05(4) Å^3 for sample 1, and $Mg_{2.17}Si_{1.01}H_{3.62}O_6$, a = 2.9853(6) Å, c = 13.9482(7) Å, V = 107.65(4) Å^3 for sample 2. The structure contains layers with many features of brucite-type units, with the layers stacked in a rhombohedral arrangement. The layers are cross linked by silicon in tetrahedral coordination and magnesium in octahedral coordination, as well as hydrogen bonds. Interlayer octahedra share edges with intralayer octahedra. Interlayer tetrahedra would share faces with intralayer octahedra. To avoid this situation, there are vacancies within the layers. There is, however, no long-range order in the occupation of these sites, as indicated by the lack of a superstructure. Selected-area electron diffraction patterns show walls of diffuse intensity similar in geometry and magnitude to those observed in short-range-ordered alloys and Hägg phases. Phase E thus appears to represent a new class of disordered silicates, which may be thermodynamically metastable.

Introduction

As part of a study of the phase equilibria of hydrous materials at pressures above 12 GPa, Kanzaki (1989) discovered a new phase, which in keeping with the nomenclature used for the four previous high-pressure, hydrous, magnesium silicates (Ringwood, Major 1967; Yamamoto, Akimoto 1974), has been named phase E. In this paper we report the unique crystal structure and crystal chemistry of two samples of phase E, which display long-range disorder of a type not previously reported in silicates.

Experimental

The initial sample of phase E (Kanzaki 1989) was synthesized at 15 GPa and 1000° C with a run duration of 15 min, using the uniaxial, split-sphere, multi-anvil apparatus. The starting material was a stoichiometric mixture of high-purity SiO_2 and $2Mg(OH)_2$. A single crystal with approximate dimensions 160 × 110 × 40 μm was used for X-ray diffraction. X-ray photographs indicated systematic absences for reflections with $-h+k+l=3n$ for hkl, which is consistent with a rhombohedral lattice, indicating that the space group is R3, $R\bar{3}$, R3m, or $R\bar{3}m$. X-ray intensity measurements were made on a Rigaku AFC5 four-circle diffractometer equipped with a rotating anode generator and a Mo target operated at 45 kV, 180 mA. Lattice constants of a = 2.959(1) Å, c = 13.844(2) Å, V = 104.98(6) Å^3 were determined from 14 reflections with 2θ between 26 and 36°. The centering algorithm employed for this study has been found to be inaccurate; therefore these values are probably consistent with those refined from powder diffraction data (a = 2.9701(1) Å, c = 13.882(1) Å, V = 106.05(4) Å^3). Neither long-exposure X-ray films nor electron diffraction studies (see below) showed any evidence for a larger unit cell. Furthermore, there were only moderate amounts of diffuse scattering observable by X-ray diffraction.

Electron microprobe analysis of the specimen at 12 sampling points showed a homogeneous chemical composition of 48.45 wt% MgO and 40.14 wt% SiO_2, yielding a total (H_2O excluded) wt% of 88.59. These analyses suffer from difficulty with low totals and the possibility of beam damage to the extremely hydrous material. No other cation with $Z \geq 11$ was detected. If closest packing of oxygen atoms is assumed, the short repeat period of the a axis and the length of the c axis allow six oxygen atoms per unit cell. There is, however, no constraint that requires this condition. If the difference of the total weight is ascribed to H_2O, the unit cell content is calculated to be $Mg_{2.27}Si_{1.26}H_{2.40}O_6$. A hemisphere of intensity data was collected for $\sin\theta/\lambda \leq 0.7$ Å^{-1}, corresponding to 6 asymmetric units of reciprocal space. The symmetry-allowed reflections were reduced to structure factors and averaged (R_{int} = 0.016) in Laue group $\bar{3}m$. Forty-four symmetry-independent reflections with $F_o > 3\sigma_F$ were obtained and used in the refinements. No absorption correction was made as $\mu_l < 9$ cm^{-1}.

* Now at Institute of Mineralogy, Petrology and Economic Geology, Faculty of Science, Tohuku University, Sendai 980, Japan
** Department of Inorganic Materials, Faculty of Engineering, Tokyo Institute of Technology, Meguro, Tokyo 152, Japan

A second sample of phase E with larger unit cell, implying a different chemical composition, was synthesized at 14 GPa and 1100° C with a run duration of 15 min from a starting mixture of $3Mg(OH)_2 + SiO_2$. The lattice constants obtained on the single-crystal diffractometer, using a more accurate centering procedure employing 20 reflections with 2θ from 25 to 40°, are a = 2.9853(6) Å, c = 13.9482(7) Å, and V = 107.65(4) Å^3. The averaged intensities ($R_{int} = 0.018$) of a total of 56 symmetry independent reflections were measured. Of these, 43 had intensities greater than the minimum observable. As above, no absorption correction was required.

The model needed to start refinement was obtained by noting that the short a-axis repeat prevents placement of atoms in any position other than 0,0,z. If Mg is placed at the origin of space group $R\bar{3}m$, the six oxygen atoms required to yield a reasonable density would form an octahedron about the Mg ion. As this Mg site is only partially filled because of the deviation from $Mg(OH)_2$ stoichiometry, its occupancy was refined. After convergence, the resulting difference Fourier maps were searched for the location of the Si site, and this cation was added to the refinement. After further refinement of occupancies, variable values of z, and temperature factors, the difference Fourier was again searched. The major feature, a positive peak at 0,0,1/2, corresponds to an interlayer magnesium octahedron. This partial atom was included, and all parameters, including anisotropic temperature factors, were refined to convergence. The interlayer magnesium position has a very low occupancy (0.013), which resulted in an instability in the thermal parameter for this atom. To overcome this diffculty, both magnesium positions were constrained to have the same temperature factor. Hydrogen atoms have not been located. All least-squares calculations were carried out with RFINE4 (Finger, Prince 1975). Scattering factors for neutral atoms were taken from the International Tables (1974).

Selected-area electron diffraction (SAED) and transmission electron microscopy (TEM) experiments were performed with a Philips 420ST microscope operated at 120 keV. The TEM samples were prepared by crushing two single crystals of sample 1 of phase E and picking up the resulting powder with holey carbon support films on copper mesh grids. All fragments that were analyzed with SAED and TEM were also analyzed using an EDAX energy-dispersive X-ray spectrometer and a Princeton Gamma-Tech System 4 analyzer, to ensure that they were phase E rather than contaminants introduced during sample preparation. Approximately fifteen fragments were studied with SAED and TEM.

X-ray Structure Results and Discussion

The structural model presented above is quite impossible on crystal chemical grounds! The intralayer Mg and interlayer Si positions are separated by only 1.8 Å; thus, these polyhedra would have to share faces, an unlikely possibility for structures formed at this pressure range (~15 GPa). It is obvious, therefore, that in any unit cell in which Si is present, the associated Mg must be absent. This coupled placement also must be randomly distributed in space, otherwise diffraction patterns would show superstructure peaks, or strong diffuse scattering. The refined models have R and weighted R factors of 0.028 and 0.022 and 0.025 and 0.023 for samples 1 and 2, respectively. Residual peaks in the difference electron density maps are less than 0.2 e/Å^3. Refined occupancy factors, positional parameters, and anisotropic temperature factors are listed in Table 1. The refined site occupancies yield compositions of $Mg_{2.08}Si_{1.16}H_{3.20}O_6$ and $Mg_{2.17}Si_{1.01}H_{3.62}O_6$ for samples 1 and 2, respectively, where change balance is used to determine the number of hydrogens. Although the X-ray composition of sample 1 differs from that obtained with the electron microprobe, it has essentially the same value for Mg/Si. Because the microprobe composition could be affected by water liberation, we will use the X-ray results to estimate the bulk composition. Relative to brucite, two substitutional paths could be considered. The first would correspond to replacing $Mg(OH)_2$ by SiO_2, whereas, the second would replace 2 MgO by SiO_2. It is found, however, that such simple substitutional models do not lead to either of the compositions studied here. The major difference between the two samples of phase E is the silicon and hydrogen contents. If these two formulae are converted to molar percentages in the ternary $MgO-SiO_2-H_2O$, the MgO content differs by 0.5%. Writing a balanced formula for the relationship, we obtain

$$E_1 + 0.42\,H_2O + 0.09\,MgO = E_2 + 0.15\,SiO_2 + 0.10\,O_2.$$

Although phase E forms at a pressure where some of the Si might be expected to be in octahedral coordination, Kanzaki et al. (1992) have shown from ^{29}Si magic angle spinning (MAS) and cross polarization MAS NMR that all Si is in tetrahedral coordination. In addition, they find the chemical shift to be significantly more negative than observed in forsterite or chondrodite, an observation consistent with the Si in phase E occurring in isolated tetrahedra, which do not share edges with Mg octahedra. Figure 1 shows one possible local arrangement for the interlayer Si with a correlated Mg vacancy. Not shown are the positions of interlayer Mg corresponding to the Mg2 site.

Selected bond distances for the structures are given in Table 2. The four-coordinated Si forms a very peculiar tetrahedron with O. This polyhedron has one normal distance of 1.66 Å and three lengths of 1.83 Å, a distance more like that of octahedrally coordinated Si. Presum-

Table 1. Positional parameters[a] and anisotropic temperature factors[b] (Å^2) for two samples of phase E

Atom	Occupancy	Multiplicity	z	$B_{\parallel}$	$B_{\perp}$
Sample 1					
Mg_1	0.664(6)	3	0	1.44(10)	1.53(8)
Mg_2	0.013(4)	3	0.5	1.44(10)	1.53(8)
Si	0.193(5)	6	0.1296(3)	0.8(1)	1.0(1)
O	1.0	6	0.2491(1)	2.3(1)	2.1(1)
Sample 2					
Mg_1	0.687(10)	3	0	1.55(9)	1.53(8)
Mg_2	0.036(6)	3	0.5	1.55(9)	1.53(8)
Si	0.169(5)	6	0.1300(3)	0.9(2)	1.1(1)
O	1.0	6	0.2503(1)	2.6(1)	2.2(1)

[a] All atoms in atomic positions 0,0,z in the average structure based on a hexagonal unit cell with space group $R\bar{3}m$. Unit-cell parameters are a = 2.9701(1) Å, c = 13.882(1) Å and a = 2.9853(6) Å, c = 13.9482(7) Å for samples 1 and 2, respectively

[b] All atoms have uniaxial thermal ellipsoids, which are presented as the B values parallel and perpendicular to the c axis ($B_{\parallel} = 4\beta_{33}/c^{*2}$, $B_{\perp} = 4\beta_{11}/a^{*2}$)

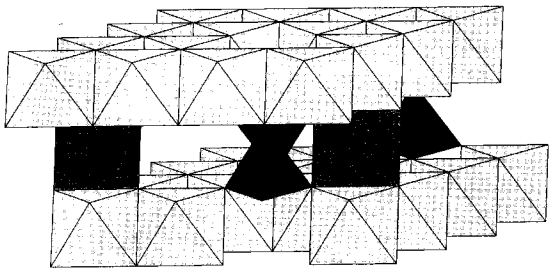

Fig. 1. Partial view of the phase E structure. Brucite-like layers of MgO_6 octahedra are crosslinked by SiO_4 tetrahedra and MgO_6 octahedra, shown in a darker shade. At the position of the tetrahedra, there is a missing cation in the brucite-like layer. The pattern of vacancies and interlayer cations is ordered locally, but has no long-range order

Table 2. Selected bond distances for the two samples of phase E

Bond	Multiplicity	Sample 1	Sample 2
Mg_1-O	6	2.076(1)	2.073(1)
Mg_2-O	6	2.062(1)	2.078(1)
Si–O	1	1.661(5)	1.675(5)
Si–O	3	1.827(1)	1.841(2)
O–O	3	2.860(3)	2.896(3)
Mg_1-Si	2	1.798(4)	1.810(4)
Mg_2-Si	2	1.791(1)	1.795(1)
Si–Si	3	2.001(4)	2.001(5)

ably, in those clusters in which tetrahedral Si is located, the absence of Mg will cause the positions of the basal oxygen atoms to be relaxed such that the long Si-O distances are shortened. The only evidence for this behavior is relatively large values for the anisotropic temperature factors. On the other hand, large temperature factors are not surprising for materials with such a large degree of disorder.

Electron Diffraction and Microscopy Results

The SAED patterns of phase E show no additional sharp diffraction spots indicative of a superstructure, confirming the X-ray diffraction results. All crystal fragments, however, produced diffuse bands of intensity between the Bragg positions in SAED patterns, as shown in Fig. 2. These bands appeared in all orientations, and their intensity was maintained even when the crystals were tilted far out of zone-axis orientations. These experiments indicate that the diffuse scattering forms complex surfaces in three dimensions.

Such three-dimensional walls of diffuse scattering are characteristic of short-range order (SRO) (Cowley 1950; Clapp, Moss 1968; Cowley 1981, Chap 17). They have been observed in a large number of materials, including Cu-Au, Cu-Pd, and Cu-Pt alloys (Cowley 1950; Ohshima, Watanabe 1973) and transition metal carbides (Hägg phases) exhibiting large deviations from stoichiometry (Billingham et al. 1972; Sauvage, Parthé 1972). Although accurate comparisons of intensities are difficult

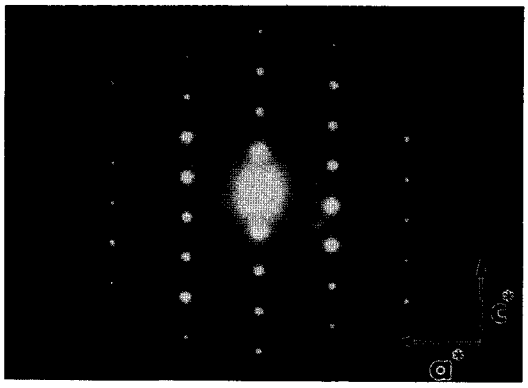

Fig. 2. An a-axis SAED pattern showing diffuse intensity between the Bragg diffraction spots. Maxima in the diffuse intensity occur where walls of diffuse scattering intersect

Fig. 3. A dark-field TEM image formed from the diffuse scattering due to SRO. The speckled contrast results from the domain structure

for electron diffraction, due to dynamical diffraction effects and differences in experimental effects, it appears that the intensity of the diffuse scattering in phase E is similar to that for other systems exhibiting SRO of large proportions of vacancies (e.g., Billingham et al. 1972). Similar to other cases (Ohshima, Watanabe 1973), intersections between the diffuse walls of intensity lead to apparent diffuse diffraction maxima in some orientations (Fig. 2), but these maxima clearly are not due to Bragg diffraction from a long-range ordered superstructure. The diffuse scattering, and hence the short-range ordering pattern, obeys the $\bar{3}\frac{2}{m}$ symmetry of the substructure.

Dark-field images formed with the diffuse intensity (Fig. 3) show the fine-scale speckling characteristic of materials with SRO (Stobbs, Chevalier 1978; Chevalier and Stobbs 1979; Howie 1988). Although the intensity variations in such dark-field images cannot be interpreted directly as the SRO domains themselves (Cowley 1973), their size indicates that the SRO domains in phase E are on the order of tens of Å in size, with a maximum dimension of approximately 50 Å.

These electron diffraction and microscopy observations confirm that phase E does not possess a long-range

superstructure, but does have short-range order. It thus appears that there is coupling between the occupancies of face-sharing cation sites, as suggested above in the discussion of the X-ray structure. However, the ordered patterns produced by this coupling extend over a range of a few tens of Å. Ideally, one could image the ordered regions and the boundaries of these domains of SRO using high-resolution TEM. Unfortunately, phase E damages very rapidly in the electron beam to a mixture of amorphous material and an unidentified, randomly oriented crystalline material; therefore, attempts to form direct images of the short-range domains failed.

Discussion

Phase E has a number of unique crystal chemical features. Both Mg and Si are distributed statistically throughout an essentially close-packed oxygen net. The only constraint is that occupied Si polyhedra cannot share faces with occupied intralayer Mg octahedra. Furthermore, all three cation positions (Mg1, Mg2, and Si) are partially occupied. Unless absolute X-ray intensities or an extremely accurate density were measured, the unit-cell contents cannot be determined.

There is an unresolved question concerning the structure of phase E under the conditions of synthesis. It is possible that the structure is short-range ordered at high P and T, but an alternative is that phase E grows with a completely disordered structure, in which the occupancies of the various crystallographic sites are truly random. If this is the case, the observed SRO must form during quenching. Obviously, it is not possible to determine with present technology which of these two possibilities is correct. It interesting to speculate, however, that a slower quench might result in a coarser domain structure. At some point, the domains might reach a size whereby they could be considered to be separate phases, with distinct structures and chemical compositions.

No matter how the observed SRO forms, it is obvious that care must be taken in the examination and interpretation of run products obtained from high-pressure regimes in the presence of large amounts of water. In the hot, wet, high-pressure environment, cation diffusion may be facilitated and these short-duration experiments thus yield extreme cation disorder within a close-packed oxygen substructure. The fact that this type of short-range order, with nearly total long-range disorder, has not been seen previously is problematic. Because phase E does not have a fixed composition or structure, it is possible that long-term annealing experiments would lead to separation of variable amounts of two, or more, phases with ordinary long-range order. Although phase E may, or may not, be a component of the mantle, these crystals represent a fascinating and unexpected new class of disordered materials with highly compliant structures.

Acknowledgements. The authors wish to acknowledge financial support of the X-ray laboratory from the National Science Foundation through instrumentation grant EAR-8618649. Crystal Synthesis work was supported by the Natural Science and Engineering Research Council of Canada grants SMI-105, CII0006947 and OGP0008394 to the late C.M. Scarfe. Electron microscopy was supported by NSF research grant EAR-8903630 and instrumentation grant EAR-8300365.

References

Billingham J, Bell PS, Lewis MH (1972) Vacancy short-range order in substoichiometric transition metal carbides and nitrides with the NaCl structure. I. Electron diffraction studies of short-range ordered compounds. Acta Crystallogr A28:602–606

Chevalier J-PAA, Stobbs WM (1979) The state of local order in quenched CuPt. Acta Metall 27:285–299

Clapp PC, Moss SC (1968) Correlation functions of disordered binary alloys. II. Phys Rev 171:754–763

Cowley JM (1950) X-ray measurement of order in single crystals of Cu_3Au. J Appl Phys 21:24–30

Cowley JM (1973) High-resolution dard-field electron microscopy. II. Short-range order in crystals. Acta Crystallogr A29:537–540

Cowley JM (1981) Diffraction physics, (2nd ed) North-Holland, Amsterdam, p 430

Finger LW, Prince E (1975) A system of Fortran IV computer programs for crystal structure computations, National Bureau of Standards Technical Note 854

Howie A (1988) Highly disordered materials. In: Buseck PR, Cowley JM, Eyring L (eds). High-resolution transmission electron microscopy and associated techniques. Oxford University Press, Oxford, pp 607–632

International Tables for X-ray Crystallography (1974) Kynoch Press, Birmingham

Kanzaki M (1989) High pressure phase relations in the system MgO-SiO_2-H_2O, EOS. Trans Am Geophys Union 70:508

Kanzaki M, Stebbins JF, Xue X (1992) Characterization of crystalline and amorphous silicates quenched from high pressure by ^{29}Si MAS NMR spectroscopy. In: Syono, Manghnani (eds). High Pressure Research: Application to Earth and Planetary Sciences (in press)

Ohshima K, Watanabe D (1973) Electron diffraction study of short-range-order diffuse scattering from disordered Cu-Pd and Cu-Pt alloys. Acta Crystallogr A29:520–526

Ringwood AE, Major A (1967) High-pressure reconnaissance investigations in the system Mg_2SiO_4-MgO-H_2O. Earth Planet Sci Lett 2:130–133

Sauvage M, Parthé E (1972) Vacancy short-range order in substoichiometric transition metal carbides and nitrides with the NaCl structure. II. Numerical calculation of the vacancy arrangement. Acta Crystallogr A28:607–616

Stobbs WM, Chevalier J-PAA (1978) The classification of short-range order by electron microscopy. Acta Metall 26:233–240

Yamamoto K, Akimoto S (1974) High-pressure and high-temperature investigations in the system Mg_2SiO_4-MgO-H_2O. J Solid State Chem 9:187–195